NUMERICAL SIMULATION AND VISUALIZATION OF THE FLOW AROUND THE DARIUS WIND TURBINE

Mi Young Lee[1] and Tetuya Kawamura[1]

A fundamental understanding of the flow around the wind turbine is important to investigate the performance of new type of wind turbine. This study presents the simulation of three dimensional flow fields around the Darius wind turbine as an example. Incompressible Navier-Stokes equations are used for this simulation. The rotating coordinate system that rotates in the same speed of the turbine is used in order to simplify the boundary condition on the blades. Additionally, the boundary fitted coordinate system is employed in order to express the shape of the blades precisely. Fractional step method is used to solve the basic equations. Third order upwind scheme is chosen for the approximation of the non-linear terms since it can compute the flow field stably even at high Reynolds number without any turbulence models. The flow fields obtained in this study are highly complex due to the three dimensionality and are visualized effectively by using the technique of the computer graphics.

Keywords: Darius Wind Turbine, Navier - Stokes Equations, Numerical Methods, Flow Visualization

1. INTRODUCTION

Recently, wind energy has received much attention as a natural energy source. Wind energy will play an important role as part of solution of world energy needs and in term of global climate change and people must act now to take advantage of the economic and environmental benefits presented by wind. The wind turbine is one of the best candidates for this purpose and most effective at supplying centralized electric power. Wind turbines have aerodynamic and aero-acoustic behaviours[1] with unique characteristics that make their prediction more challenging in many ways than already complicated aero-acoustic problems such as rotorcraft or propeller noise.

While there are many kinds of wind turbine, they can be classified into two types if we look at the axis of the turbine, i.e. horizontal axis type and vertical axis type. The typical example of the former is the propeller turbine that is the most widely used for generating electricity. The disadvantage of this type is that the performance of the turbine is greatly affected by the direction of the wind. Thus, it must be set at the area where the wind is blowing almost from the constant direction or it is required to mount special equipment similar to the tail of an airplane which moves the wind turbine to the best direction. On the other hand, the vertical axis type[2] is free from this disadvantage, and it can be rotated by wind blowing from any direction. The Darius turbine is a typical example of a vertical axis type wind turbine and it is also suitable for generating electricity because of its high performance. The main disadvantage of the Darius turbine is that it cannot start to rotate from rest. In order to overcome this disadvantage, a new type of the wind turbine has been developed which combines the Darius turbine and the Savonius turbine, both of which have the same axis of rotation. The role of the Savonius turbine is to help whole system to move from rest.

We are now looking at potentiality of the wind turbine of the vertical axis types and try to investigate the performance of the turbine of this kind. The objective of the present study is to simulate and visualize numerically the flow field around the Darius turbine and the modified Darius turbine in order to show the effectiveness of the

Received: July 20, 2004, Accepted: January 31, 2005.

1 Graduate school of humanities and sciences, Ochanomizu University, 2-1-1 Ootsuka, Bunkyo-ku, Tokyo 112-8610, JAPAN

numerical method and to obtain fundamental data for their design. No explicit turbulence model is incorporated into the present study.

2. NUMERICAL METHOD

2.1 BASIC EQUATIONS

Since the flow is assumed to be highly three-dimensional, the three-dimensional incompressible Navier-Stokes equations are used for the simulation. If we choose the z-direction as the rotational axis[3, 4], the equations become

$$\frac{\partial U}{\partial X}+\frac{\partial V}{\partial Y}+\frac{\partial W}{\partial Z}=0 \tag{1}$$

$$\frac{\partial u}{\partial t}=-\frac{\partial P}{\partial X}\cos\theta-\frac{\partial P}{\partial Y}\sin\theta+A \tag{2}$$

$$\frac{\partial v}{\partial t}=\frac{\partial P}{\partial X}\sin\theta-\frac{\partial P}{\partial Y}\cos\theta+B \tag{3}$$

$$\frac{\partial w}{\partial t}=-\frac{\partial P}{\partial Z}+C \tag{4}$$

where

$$A=-U\frac{\partial u}{\partial X}-V\frac{\partial u}{\partial Y}-W\frac{\partial u}{\partial Z}+\frac{1}{Re}\left(\frac{\partial^2 u}{\partial X^2}+\frac{\partial^2 u}{\partial Y^2}+\frac{\partial^2 u}{\partial Z^2}\right) \tag{5}$$

$$B=-U\frac{\partial v}{\partial X}-V\frac{\partial v}{\partial Y}-W\frac{\partial v}{\partial Z}+\frac{1}{Re}\left(\frac{\partial^2 v}{\partial X^2}+\frac{\partial^2 v}{\partial Y^2}+\frac{\partial^2 v}{\partial Z^2}\right) \tag{6}$$

$$C=-U\frac{\partial w}{\partial X}-V\frac{\partial w}{\partial Y}-W\frac{\partial w}{\partial Z}+\frac{1}{Re}\left(\frac{\partial^2 w}{\partial X^2}+\frac{\partial^2 w}{\partial Y^2}+\frac{\partial^2 w}{\partial Z^2}\right) \tag{7}$$

Here, X, Y and Z are the Cartesian coordinates of the rotational system and x, y and z are those of the stational system. The relations between these coordinates are

$$X=x\cos\theta-y\sin\theta \tag{8}$$

$$Y=x\sin\theta+y\cos\theta \tag{9}$$

$$Z=z \tag{10}$$

where $\theta=\omega t$ is the angle between two coordinate systems. ω is the angular velocity of the rotating system (fig. 1). Similarly, U, V and W are the velocity components of the rotational system and u, v and w are those of the stational system. In this case, the following relations hold:

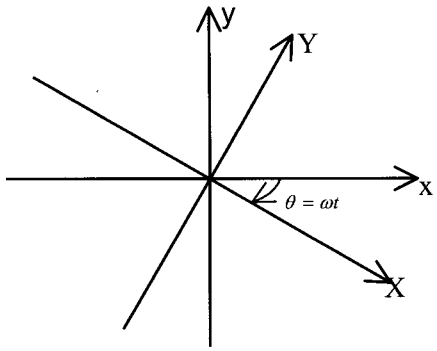

Fig. 1 Rotational coordinate system

$$U=u\cos\theta-v\sin\theta-\omega Y \tag{11}$$

$$V=u\sin\theta+v\cos\theta+\omega X \tag{12}$$

$$W=w \tag{13}$$

In the computation, all the variables in equations are replaced to non-dimensional counterparts.

2.2 NUMERICAL METHOD

These equations are solved by the fractional step method.[2] The outline of this method is as follows: At first, the pressure terms are dropped from the momentum equations (2), (3) and (4) and they are integrated by the Euler explicit method to obtain temporal velocity components.

$$u^*=u+\Delta tA \tag{14}$$

$$v^*=v+\Delta tB \tag{15}$$

$$w^*=w+\Delta tC \tag{16}$$

The temporal velocity is used to calculate the source term of the Poisson equation, which determines the pressure field.

$$\frac{\partial^2 P}{\partial X^2}+\frac{\partial^2 P}{\partial Y^2}+\frac{\partial^2 P}{\partial Z^2}=\frac{1}{\Delta t}\left(\frac{\partial U^*}{\partial X}+\frac{\partial V^*}{\partial Y}+\frac{\partial W^*}{\partial Z}\right) \tag{17}$$

In equation (17), U^*, V^*, and W^* are computed from U^*, V^*, W^* by using equation (11), (12), (13). The velocity components at next time step are computed from

$$u^{n+1}=u^n-\Delta t\left(\frac{\partial P}{\partial X}\cos\theta+\frac{\partial P}{\partial Y}\sin\theta\right) \tag{18}$$

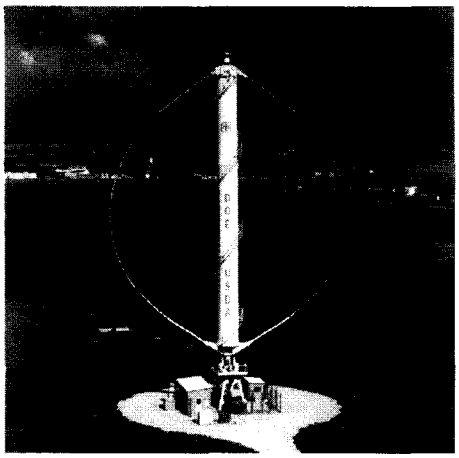

Fig. 2 Darrieus Vertical-Axis Wind Turbine (DOE/Sandia's 34-meter)

$$v^{n+1} = v^n - \Delta t\left(-\frac{\partial P}{\partial X}\sin\theta + \frac{\partial P}{\partial Y}\cos\theta\right) \tag{19}$$

$$w^{n+1} = w^n - \Delta t\frac{\partial P}{\partial Z} \tag{20}$$

These equations are transformed into computational plane through using the generalized coordinate system

$$X = X(\xi,\eta,\zeta) \tag{21}$$

$$Y = Y(\xi,\eta,\zeta) \tag{22}$$

$$Z = Z(\xi,\eta,\zeta) \tag{23}$$

which enable us to employ the curvilinear grids in physical plane.[3] For example, the first derivative of the pressure with respect to x is transformed into

$$\frac{\partial P}{\partial X} = \frac{1}{J}\left(\left(Y_\eta Z_\zeta - Y_\zeta Z_\eta\right)P_\xi + \left(Y_\zeta Z_\xi - Y_\xi Z_\zeta\right)P_\eta + \left(Y_\xi Z_\eta - Y_\eta Z_\xi\right)P_\zeta\right) \tag{24}$$

where J is the Jacobian of the transformation and is expressed by

$$J = X_\xi Y_\eta Z_\zeta + Y_\xi Z_\eta X_\zeta + Z_\xi X_\eta Y_\zeta - Z_\xi Y_\eta X_\zeta - X_\xi Z_\eta Y_\zeta - Y_\xi X_\eta Z_\zeta \tag{25}$$

The transformed equations are solved by the finite difference method. All the spatial derivatives except nonlinear terms are approximated by the central differences. Nonlinear terms are approximated by the third order upwind scheme[5], e.g.

$$f\frac{\partial U}{\partial \xi} = f\frac{-U_{i+2} + 8(U_{i+1} - U_{i-1}) + U_{i-2}}{12\Delta\xi} + |f|\frac{U_{i+2} - 4U_i + 6U_i - 4U_{i-1} + U_{i-2}}{12\Delta\xi} \tag{26}$$

since it gives solutions without any turbulence models even at considerably high Reynolds number.

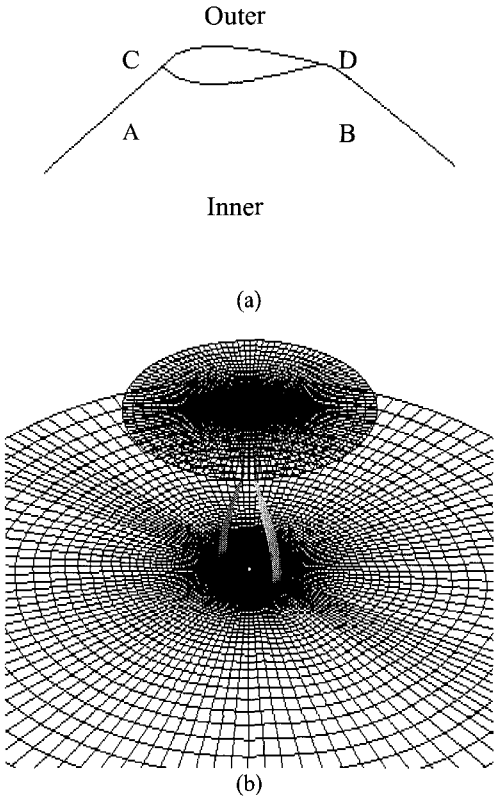

Fig. 3 Grid for computation (a) Grid lines passing the blade, (b) Grid for the Darius rotor (horizontal plane)

2.3 GRID FOR THE DARIUS TURBINE

Fig. 2 shows the Darrieus vertical-axis wind turbine (DOE/Sandia's 34-meter). It can produce more than half the electricity needed to power the local community, but it is a research and development tool only.

At first, two-dimensional grid system in the plane perpendicular to the rotational axis is generated. As is shown in Fig. 3(a), this region is divided into two regions, i.e. inner region and outer region. The inner side of the blade is located at AB while the outer side is located at CD in this figure. The grid systems in both regions are obtained by deforming the grids of the polar coordinate. The shape of the blade is determined by using Joukovski transformation. After obtaining the grids in each cross section, they are piled in the axial direction to get whole grid system. Fig. 3(b) shows two blades and the part of the grid system mainly used in this study. The grid points is $120 \times 63 \times 42$ in circumferential, radial and axial direction respectively. The far boundary in each cross section is the circle of radius 10R where R is the distance between the axis and the blade of the turbine. The lower and upper boundary locates z=0 and z=2L where L is the height of the turbine.

2.4 INITIAL AND BOUNDARY CONDITIONS

Initially, the flow is assumed to be uniform in whole region. The flow is also assumed to be uniform at far boundaries except the outflow boundary where the velocity is determined by the extrapolation. The pressure gradient at far boundaries is assumed to be zero. No-slip condition is imposed on the blade. The pressure on the blade is determined by substituting the velocity condition (no-slip) into the momentum equations. The shape of the Darius turbine is symmetric with respect to the center plane, i.e. the plane that is perpendicular to the axis of the turbine and passes the midpoint of the axis. Therefore only upper half region is used for the computations and the symmetric boundary condition is imposed on the center plane.

3. NUMERICAL RESULTS

Examples of the results obtained by the present numerical method are shown here. The speed of the flow at far boundary is assumed to be 5m/s and the kinematics' viscosity of the fluid is 0.03 m^2/sec. This value is two thousand times as large as molecular viscosity of the air. However this is reasonable since the effective viscosity (i.e. eddy viscosity) of the air is not so small due to the effect of turbulence. In Figs 4-6, the wind comes from left side of each figure.

Fig. 4(a) shows the velocity vectors for the Darius turbine in the center plane at various angles of attack, Fig. 4(b) shows the pressure contour lines

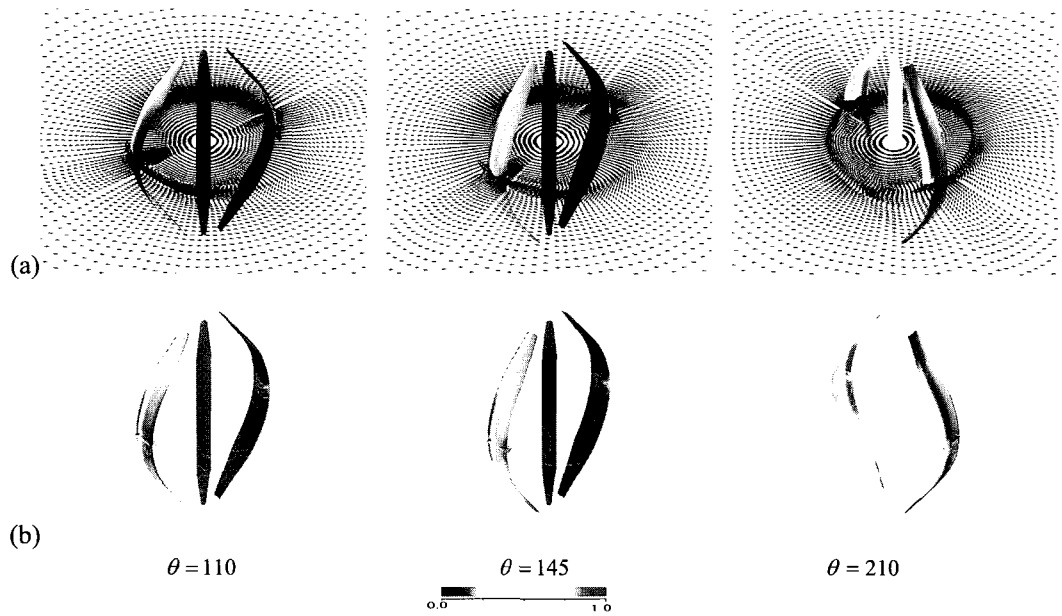

Fig. 4 Velocity vectors (a) and pressure contour lines (b) for the Darius turbine in the center plane at various angle of attack θ (Colors bar shows the surface value of the blades)

corresponding to Fig. 4(a). In this figure, pressure distributions on the blades are also shown.

Computational studies are being utilized to predict the load control and power gain that can be expected from the various devices and to optimize device size and placement. Blades[6] are the only wind turbine component designed and manufactured uniquely for wind energy applications. The challenge to be met is to create the scientific knowledge base and engineering tools to enable designers to maximize performance at the lowest possible cost. This task enables the wind industry to stretch rotors to greater swept areas and improve rotor blade designs[7] for increased energy capture, thus enabling profitable wind turbine operation in previously uneconomic wind regimes. Flow visualization by movies or animations is desirable when the flow is highly three dimensional and complex.

Fig. 5(a) shows velocity vectors for the modified Darius turbine in the center plane at two different attack angles, for the modified Darius turbine that has the Savonius rotors inside.

Fig. 6 shows streamlines and pressure distribution on the inner blades and outer blades of the Darius turbine (a) and modified Darius turbine (b). In this figure, pressure distributions on the blades are also shown.

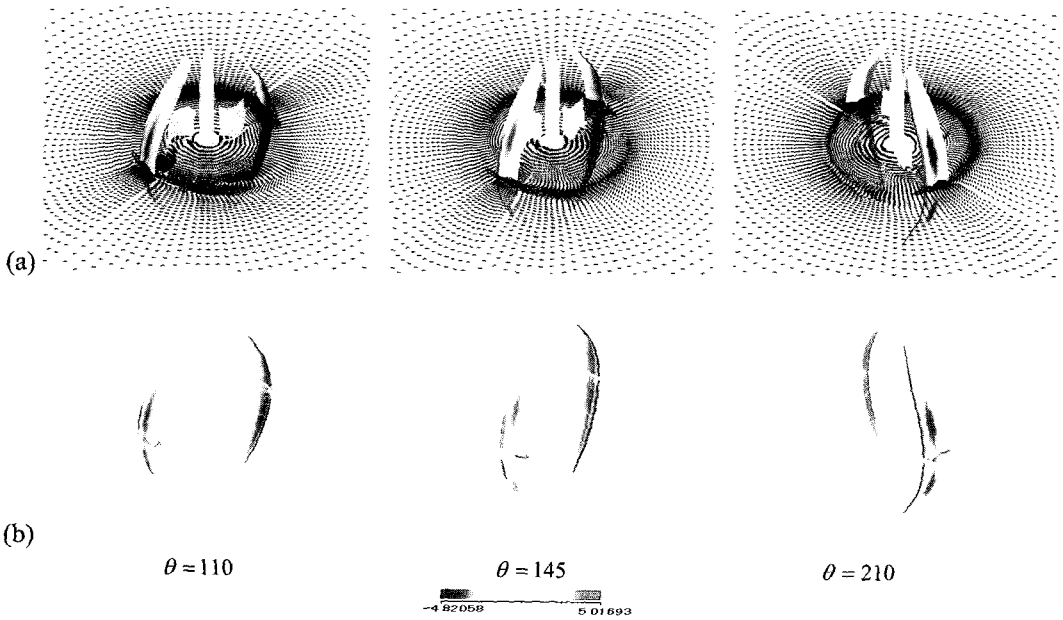

Fig. 5 Velocity vectors (a) and pressure contour lines (b) for the modified Darius turbine in the center plane

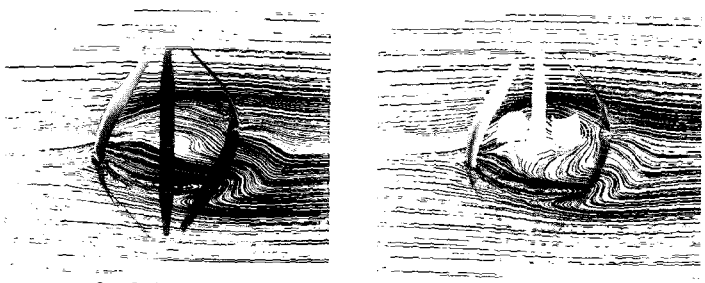

Fig. 6 Streamlines and pressure distribution on the inner blades and outer blades of the Darius turbine (a) and modified Darius turbine (b).

4. SUMMARY

In this study, complex flow field around the Darius turbines rotating stationally are simulated by solving the three dimensional incompressible Navier-Stokes equation numerically. The rotating coordinate system is employed so that the boundary conditions on the blades of the rotor become simple. In order to impose the boundary condition on the blades precisely, the boundary fitted coordinate system is employed. Fractional step method is used to solve the basic equations.

The complex flow fields due to both three dimensionality of the geometry of the turbine and the rotation of the turbine are obtained and they are visualized effectively by using the technique of the computer graphics. From these results, we can conclude that the numerical method developed in this study become the promising tools for the design of the new wind turbine.

5. REFERENCES

[1] Morris, P.J., Long, L.N. and Brentner K.S., 2004, "An Aeroacoustic Analysis of Wind Turbines," *AIAA,* pp. 2004-1184.

[2] Kadlec, E.G., 1979, "Characteristics of Future Vertical-Axis Wind Turbines," *SLA-79-1068*, Sandia Laboratories.

[3] Yanenko, N.N, 1971, *The Method of ractional Step*, Springer-Verlarg.

[4] Thompson, J.F., Warzi, Z.U.A. and Mastin, C.W., 1985, *Numrical Grid Generation*, Foundations and Applications, North-Holland.

[5] Kawamura, T and Kuwahara, K, 1984, *AIAA,* pp. 84-0340.

[6] Blackwell, B.F. and Reis, G.E., 1974, "Blade Shape for a Troposkien Type of Vertical-Axis Wind Turbine," *SLA-74-0154.*

[7] Paraschivoiu, I., *Wind Turbine Design-With Emphasis on Darrieus Concept*, Polytechnic international Press, 2002.